BEST COPY AVAILABLE

Observing and Learning Chaotic Phenomena from Chua's Circuit

R. N. Madan
Office of Naval Research

Abstract

The ubiquitous phenomenon of *Chaos* is introduced by *experimentally* observing the bifurcation phenomena from Chua's circuit as a single parameter, the tuning resistance R, is varied. Complete details for building a robust experimental Chua's circuit are given. The entire circuit takes less than 30 minutes to hook up and cost less than $5. This experimental Chua's circuit uses only a BiFET dual op amp IC, and linear passive elements. Finally, a picture book documentation of the various bifurcation episodes observed from this circuit is given, thereby illustrating the Hopf bifurcation phenomenon, the universal period-doubling route to chaos, and 2 examples of *strange attractors*.

1 Introduction

The objective of this tutorial paper is to provide an elementary introduction to *chaos* from an *experimental* point of view. We will conduct our experiments with the help of Chua's circuit [1, 2, 3], shown in Fig.1. This circuit contains 2 linear passive capacitors, 1 linear passive inductor, 1 linear passive resistor, and a 2-terminal nonlinear resistor whose v_R-i_R characteristic is shown in Fig. 2. We have chosen Chua's circuit as a vehicle for observing and learning chaos for three reasons. *First* it has been proved [4] that this circuit is the simplest autonomous electronic circuit which is endowed with an extremely rich repertoire of complicated nonlinear bifurcation phenomena, including chaos. The term "autonomous" means that the circuit is not driven by any ac signals. Since the resistance

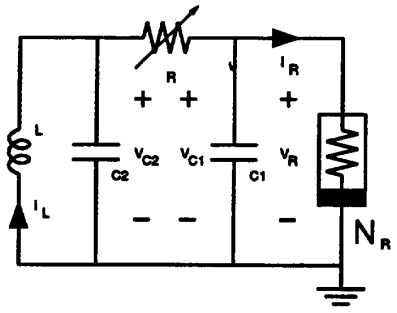

Figure 1: Chua's circuit

R, inductance L, and capacitances C_1 and C_2 in Chua's circuit are positive numbers, it is clear that in order for this circuit to oscillate, let alone become chaotic, the nonlinear resistor must be *active* in the sense that its v_R-i_R characteristic must include some regions in the *2nd*, or the *4th* quadrant, where the product $v_R \cdot i_R$ is *negative*, thereby supplying power to the passive elements. However, since no physical device can supply an infinite amount of power, any physically realizable v_R-i_R characteristic must be *eventually passive* in the sense that the v_R-i_R curve must lie in the *1st* and *3rd* quadrants, for sufficiently large values of v_R. This requirement explains why the two outermost segments have a positive slope, even though, as we will see in our experiments, only the 3 inner segments with the *negative* slopes are used in generating the chaotic phenomena, as originally conceived and stipulated by Chua in his design [4]. The *second* reason for choosing Chua's circuit is its low cost (less than $5) and robustness [5]: the experimental circuit to be described in *section 2* can be hooked up in less than 30 minutes and will oscillate in a chaotic manner as soon as the battery (power supply for the nonlinear resistor) is connected. In this paper, we will define an autonomous circuit as chaotic if its associated state variables exhibit an oscillatory motion which is neither periodic nor almost periodic in the sense that the *frequency spectrum* is *continuous*, and not discrete.

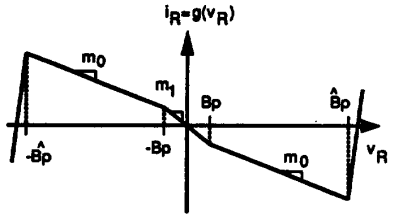

Figure 2: The v_R-i_R characteristic of Chua's diode

The *third* reason for choosing Chua's circuit is its recognition among the nonlinear dynamics community as a simple yet extremely general paradigm for chaos. Indeed with more than 40 papers published on various aspects of Chua's circuit, and with the forthcoming 2-volume Special Issue devoted exclusively to this circuit [6, 7], Chua's circuit has become the single most studied and well-understood paradigm for chaos.

2 Building the Experimental Chua's Circuit

The only circuit element in Chua's circuit which is not available as standard off-the-shelf components is the nonlinear resistor having the *non-monotonic* active v_R-i_R characteristic shown in Fig. 2. Prior to the pioneering works by Chua in the mid sixties [8, 9, 10, 11, 12] , such characteristics are generally dismissed as hypothetical. There are now numerous systematic techniques for synthesizing *prescribed* v_R-i_R characteristics using standard off-the-shelf components such as diodes, transistors, op amps, etc. To distinguish these *artificially* synthesized circuit elements from other off-the-shelf nonlinear devices (e.g. neon bulbs, tunnel diodes, etc.), we will henceforth adopt Kennedy's terminology [5] and refer to any artificially synthesized 2-terminal resistor characterized by an eventually-passive non-monotonic active v_R-i_R characteristic as *Chua's diode*.

Several circuit realizations of Chua's diode having the v_R-i_R characteristic shown in Fig. 2 are available. We will choose the most robust realization given by Kennedy [5], which we reproduce in Fig.

0-7803-0510-8/92$03.00 ©1992IEEE

3. Observe that the circuit which realizes Chua's diode is enclosed within the one-port N_R: it requires 2 op amps (powered by two 9V batteries) and 6 linear positive resistors. The 2 opamps are available in a *single* 8-pin package (e.g. Analog Devices AD712 dual BiFET opamp). The complete component list for this circuit is given below. In addition to the components listed, a bypass capacitor C of at least 0.1μF connected to each power supply as close to the op amp as possible is recommended, as shown in Fig. 3. The purpose of these capacitors is to maintain the power supplies at a steady dc voltage.

Figure 6(a) shows only the portion of the $v_R - i_R$ characteristic where the chaotic phenomena are observed. To demonstrate the eventual passivity of Chua's diode, we increase the amplitude of the triangular tracing waveform and obtained the 5-segment $v_R - i_R$ characteristic shown in Fig. 6(b).

We remark that a Chua's diode *integrated circuit* has recently been built [13] which obviates the need for a separate realization. Such IC's, when produced in large quantities, would cost less than that of a single op amp, thereby making Chua's circuit a truly low-cost generator of chaotic signals.

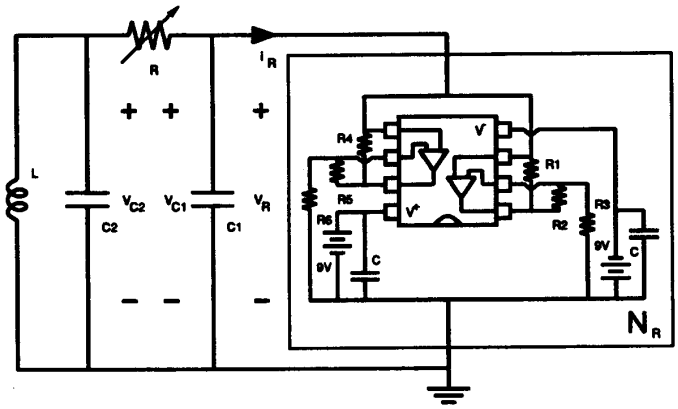

Figure 3: Practical realization of Chua's diode using an eight-pin dual op amp integrated circuit

2.1 Component list

Element	Description	Value	Tolerance
A_1	Op amp ($\frac{1}{2}$ AD712, TL082, or equivalent)		
R_1	$\frac{1}{4}$W Resistor	220 Ω	±5%
R_2	$\frac{1}{4}$W Resistor	220 Ω	±5%
R_3	$\frac{1}{4}$W Resistor	2.2 kΩ	±5%
A_2	Op amp ($\frac{1}{2}$ AD712, TL082, or equivalent)		
R_4	$\frac{1}{4}$W Resistor	22 kΩ	±5%
R_5	$\frac{1}{4}$W Resistor	22 kΩ	±5%
R_6	$\frac{1}{4}$W Resistor	3.3 kΩ	±5%
C_1	Capacitor	10 nF	±5%
R	Potentiometer	2 kΩ	
C_2	Capacitor	100 nF	±5%
L	Inductor (TOKO type 10RB or equivalent)	18 mH	± 10%

To demonstrate how small a package we can pack the circuit elements inside N_R, Fig. 4 shows a photograph of the actual circuit, where the black cube (measures $1\frac{1}{2}$cm $\times 1\frac{1}{2}$cm $\times 2$ cm) on the right is a physically realized Chua's diode.

The v_R-i_R characteristic of this Chua's diode circuit realization can be measured by connecting N_R in series with a small current-sensing resistor R_s, as shown in Fig. 5. This resistor is used to measure the current i_R which flows into N_R when a voltage v_R is applied across its terminals. An appropriate choice of R_s in this measurement is 100Ω. The current i_R in this case causes a voltage $v_{i_R} = -100 i_R$ to appear across the sensing resistor. Hence, we can measure the $v - i$ characteristic of N_R by applying a voltage v_s as shown and plotting v_{i_R} (proportional to $-i_R$) versus v_R to the X-input of an oscilloscope in X-Y mode. The resulting characteristic for the components listed in the table is shown in Fig. 6. Note that we have plotted $-v_{i_R}$ versus v_R; this is possible if the oscilloscope permits inversion of the Y-input in the $X - Y$ mode.

3 Tuning R to Observe Bifurcation Phenomena

For this introductory paper, we will fix all circuit parameters except the resistor R, which will be varied continuously from $R = 2100\Omega$ down to $R = 1545\Omega$. A $2k$ miniature potentiometer with a tuning screw for varying R is recommended. The following experimental results are collected in the form of a picture book, which documents the oscilloscope observations for each value of R where a bifurcation occurs (i.e., the $v_{C_1} - v_{C_2}$ trajectory undergoes a sudden change in its *qualitative behavior*). Each bifurcation episode shows the waveform of v_{C_1} on the left, its measured frequency spectrum in the center, and the associated $v_{C_1} - v_{C_2}$ trajectory (Lissajous figure) on the right. The parameter values corresponding to these measurements are given below each picture.

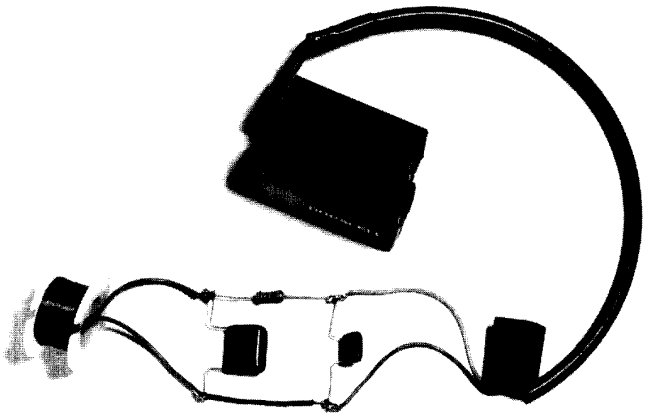

Figure 4: Photograph of the experimental Chua's circuit

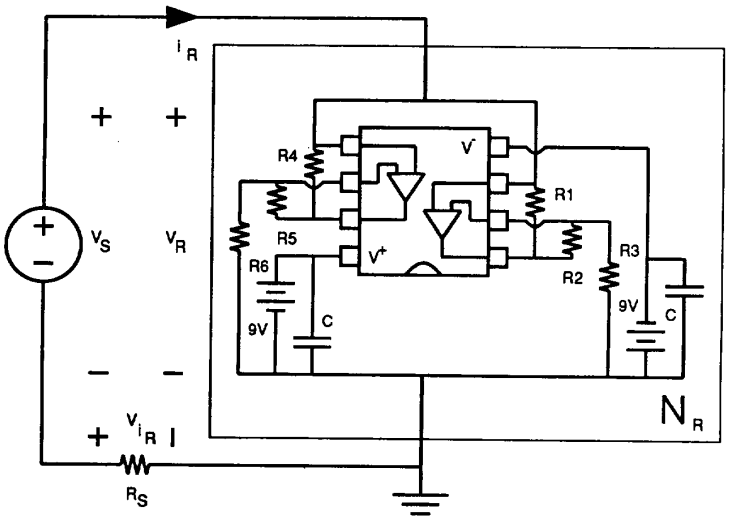

Figure 5: The $v - i$ characteristic of negative resistor N_R can be measured by applying a triangular voltage waveform v_S to the series combination of N_R and a small current-sensing resistor R_S. Plot $-v_{i_R}(\propto i_R)$ versus v_R. The eight-pin dual op amp package is shown from above in schematic form. The reference end of the package is indicated by a dot or a semicircle (shown here).

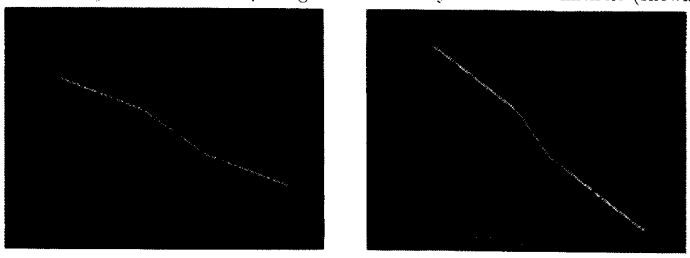

(a) (b)

Figure 6: Measured $v - i$ characteristic of negative resistor. (a) v_S is a triangular waveform with zero dc offset, amplitude 7V peak-to-peak, and frequency 30 Hz. Horizontal axis: v_R (1V/div); Vertical axis: $-v_{i_R}$ (100mV/div); (b) v_S is a triangular waveform with zero dc offset, amplitude 15V peak-to-peak, and frequency 30 Hz. Horizontal axis: v_R (2V/div); Vertical axis: $-v_{i_R}$ (100mV/div).

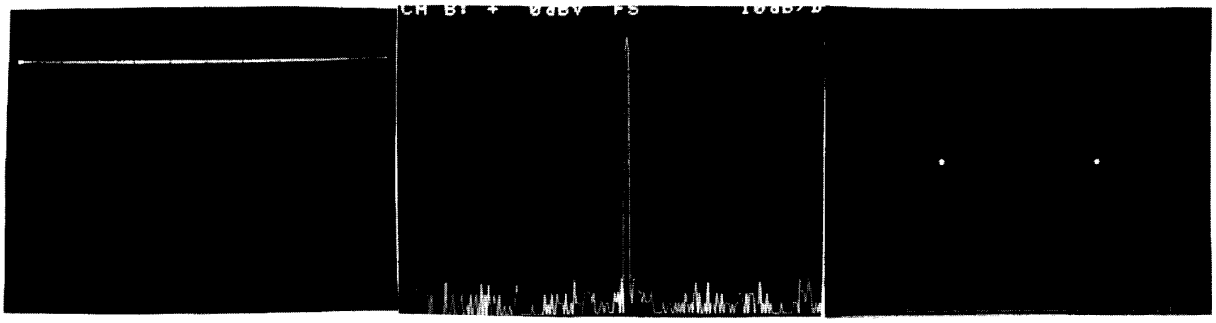

(a) (b) (c)

Figure 7: $R = 2100\Omega$, $C_1 = 10\text{nF}$, $C_2 = 100\text{nF}$, $L = 18\text{mH}$, $m_1 = -\frac{25}{33}\text{mS}$, $m_0 = -\frac{4}{22}\text{mS}$.

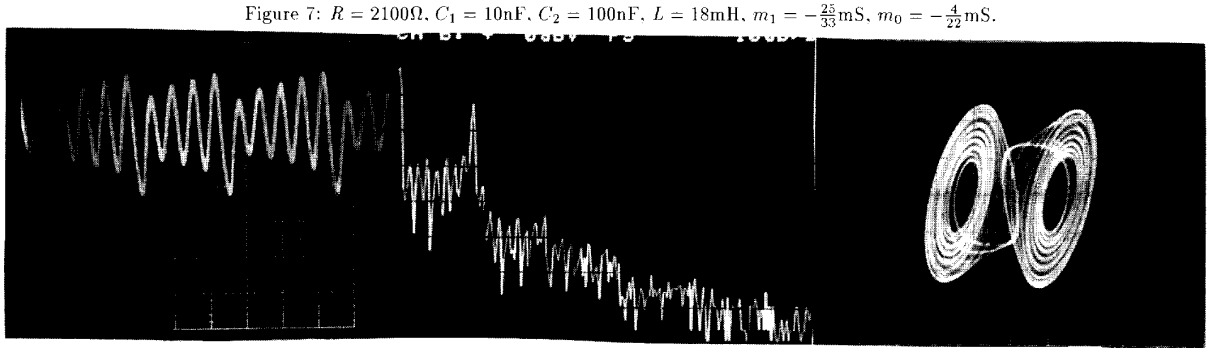

(a) (b) (c)

Figure 8: $R = 1936\Omega$, $C_1 = 10\text{nF}$, $C_2 = 100\text{nF}$, $L = 18\text{mH}$, $m_1 = -\frac{25}{33}\text{mS}$, $m_0 = -\frac{4}{22}\text{mS}$.

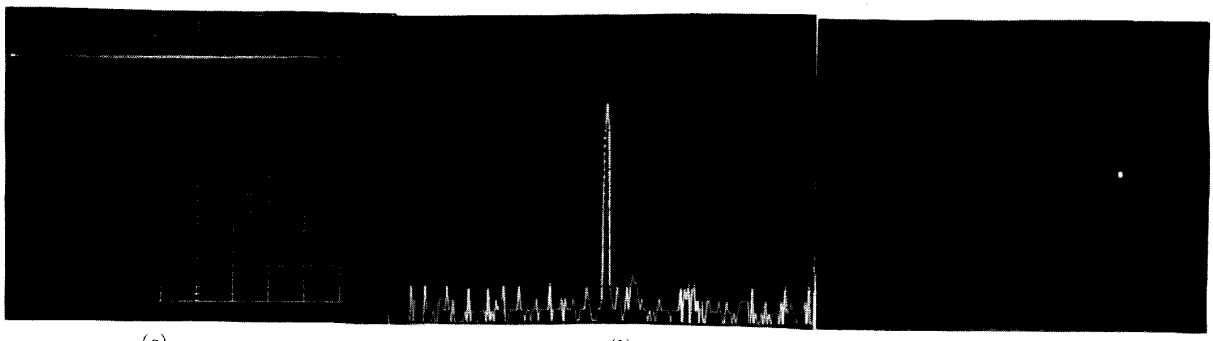

(a) (b) (c)

Figure 9: $R = 2100\Omega$, $C_1 = 10\text{nF}$, $C_2 = 100\text{nF}$, $L = 18\text{mH}$, $m_1 = -\frac{25}{33}\text{mS}$, $m_0 = -\frac{4}{22}\text{mS}$.

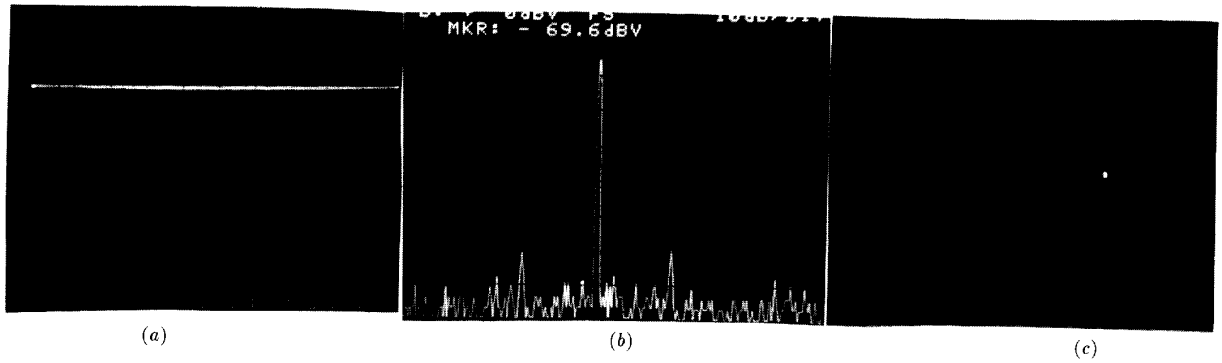

(a) (b) (c)

Figure 10: $R = 2019\Omega$, $C_1 = 10\text{nF}$, $C_2 = 100\text{nF}$, $L = 18\text{mH}$, $m_1 = -\frac{25}{33}\text{mS}$, $m_0 = -\frac{4}{22}\text{mS}$.

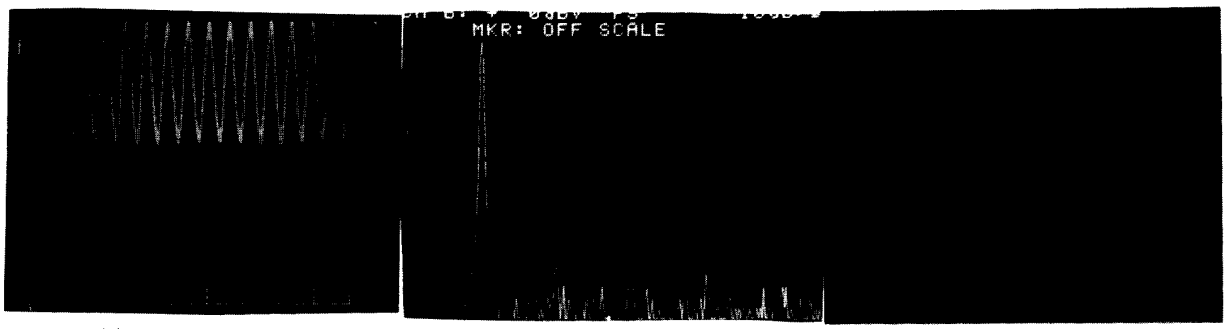

(a) (b) (c)

Figure 11: $R = 2018\Omega$, $C_1 = 10\text{nF}$, $C_2 = 100\text{nF}$, $L = 18\text{mH}$, $m_1 = -\frac{25}{33}\text{mS}$, $m_0 = -\frac{4}{22}\text{mS}$.

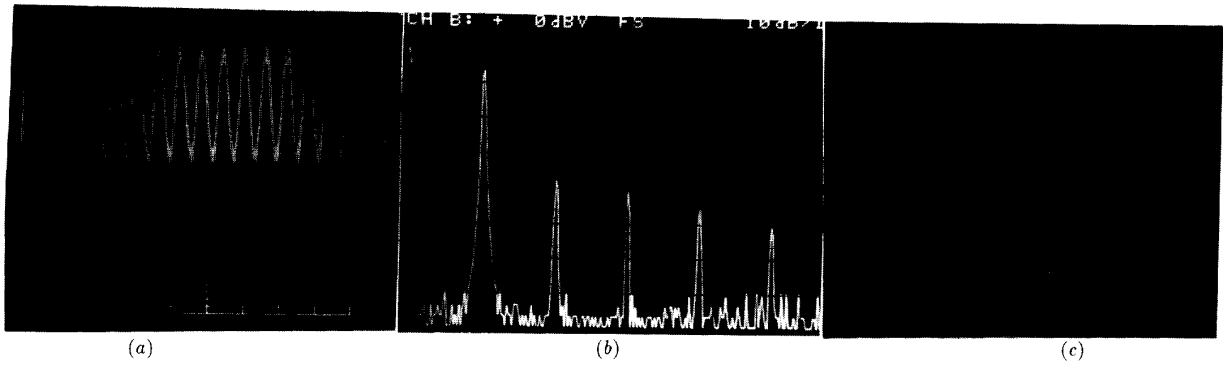

(a) (b) (c)

Figure 12: $R = 1977\Omega$, $C_1 = 10\text{nF}$, $C_2 = 100\text{nF}$, $L = 18\text{mH}$, $m_1 = -\frac{25}{33}\text{mS}$, $m_0 = -\frac{4}{22}\text{mS}$.

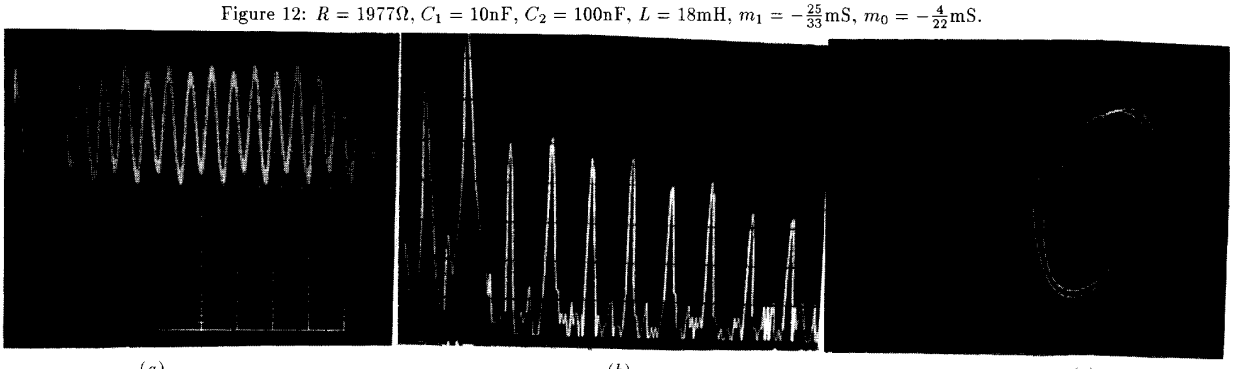

(a) (b) (c)

Figure 13: $R = 1966\Omega$, $C_1 = 10\text{nF}$, $C_2 = 100\text{nF}$, $L = 18\text{mH}$, $m_1 = -\frac{25}{33}\text{mS}$, $m_0 = -\frac{4}{22}\text{mS}$.

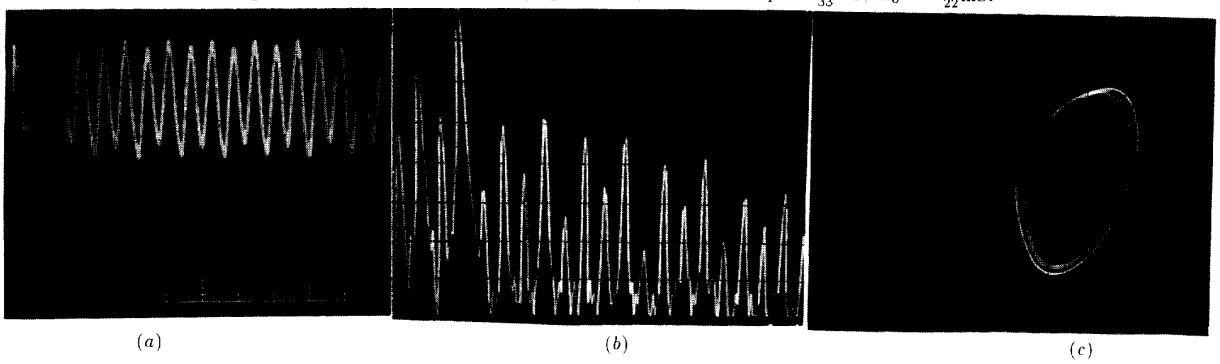

(a) (b) (c)

Figure 14: $R = 1962\Omega$, $C_1 = 10\text{nF}$, $C_2 = 100\text{nF}$, $L = 18\text{mH}$, $m_1 = -\frac{25}{33}\text{mS}$, $m_0 = -\frac{4}{22}\text{mS}$.

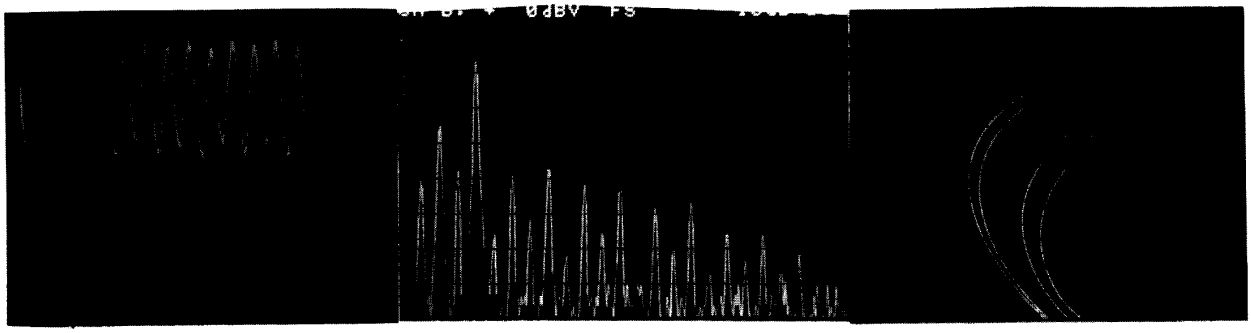

(a) (b) (c)

Figure 15: $R = 1962\Omega$, $C_1 = 10\text{nF}$, $C_2 = 100\text{nF}$, $L = 18\text{mH}$, $m_1 = -\frac{25}{33}\text{mS}$, $m_0 = -\frac{4}{22}\text{mS}$.

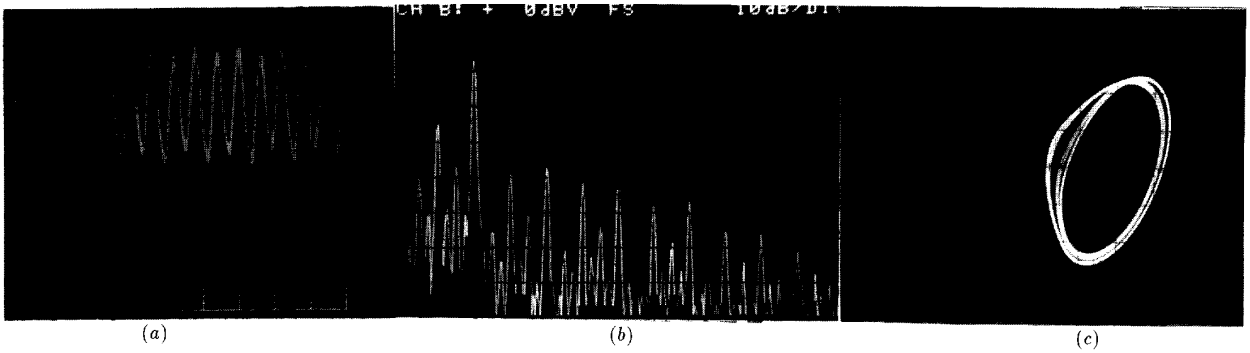

(a) (b) (c)

Figure 16: $R = 1961\Omega$, $C_1 = 10\text{nF}$, $C_2 = 100\text{nF}$, $L = 18\text{mH}$, $m_1 = -\frac{25}{33}\text{mS}$, $m_0 = -\frac{4}{22}\text{mS}$.

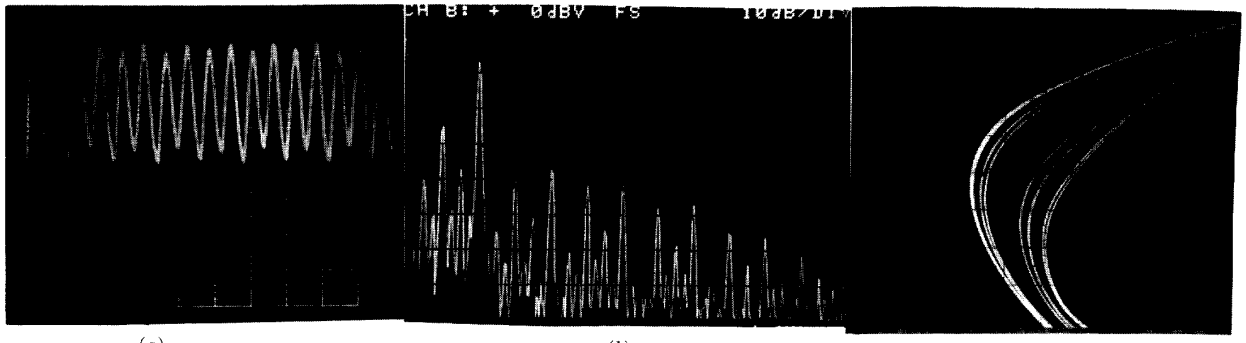

(a) (b) (c)

Figure 17: $R = 1961\Omega$, $C_1 = 10\text{nF}$, $C_2 = 100\text{nF}$, $L = 18\text{mH}$, $m_1 = -\frac{25}{33}\text{mS}$, $m_0 = -\frac{4}{22}\text{mS}$.

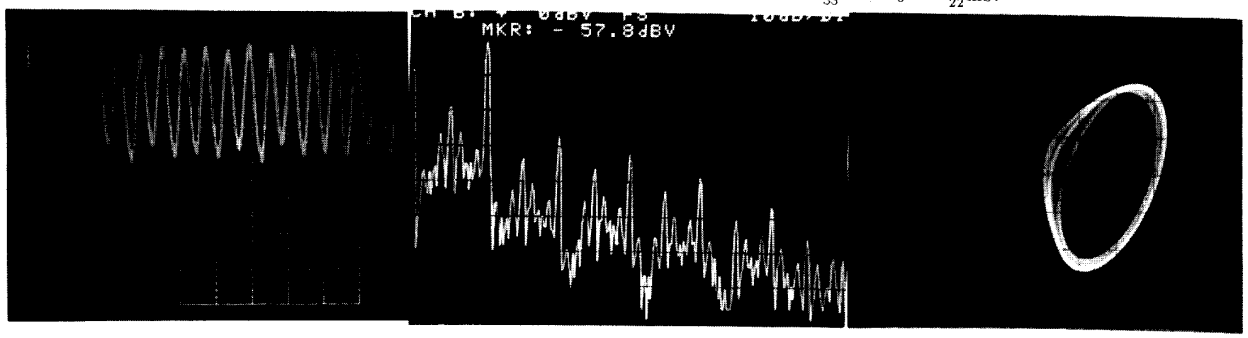

(a) (b) (c)

Figure 18: $R = 1958\Omega$, $C_1 = 10\text{nF}$, $C_2 = 100\text{nF}$, $L = 18\text{mH}$, $m_1 = -\frac{25}{33}\text{mS}$, $m_0 = -\frac{4}{22}\text{mS}$.

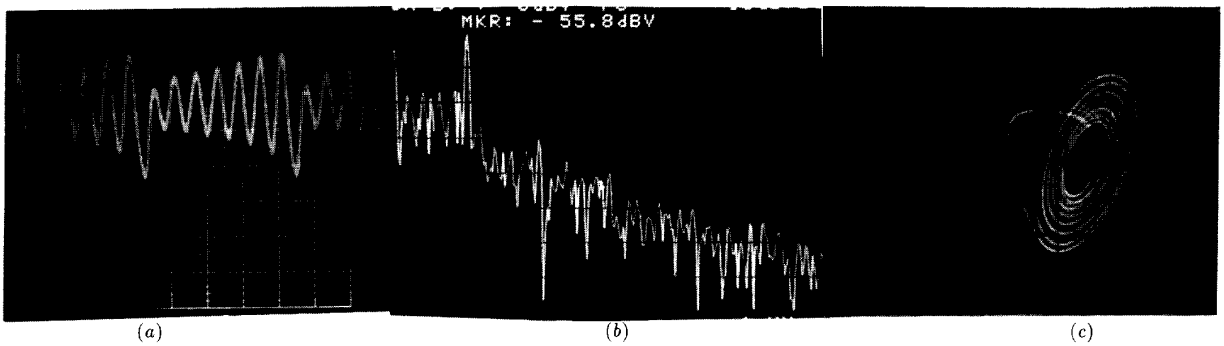

(a) (b) (c)

Figure 19: $R = 1936\Omega$, $C_1 = 10\text{nF}$, $C_2 = 100\text{nF}$, $L = 18\text{mH}$, $m_1 = -\frac{25}{33}\text{mS}$, $m_0 = -\frac{4}{22}\text{mS}$.

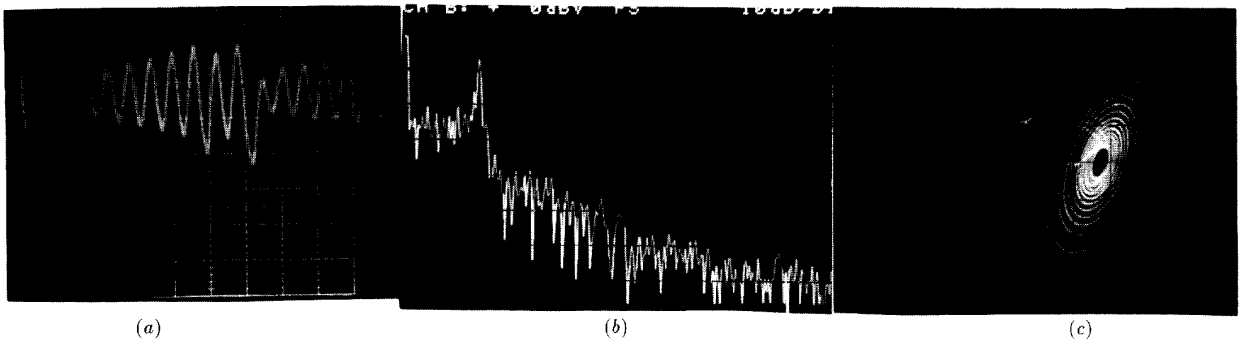

(a) (b) (c)

Figure 20: $R = 1931\Omega$, $C_1 = 10\text{nF}$, $C_2 = 100\text{nF}$, $L = 18\text{mH}$, $m_1 = -\frac{25}{33}\text{mS}$, $m_0 = -\frac{4}{22}\text{mS}$.

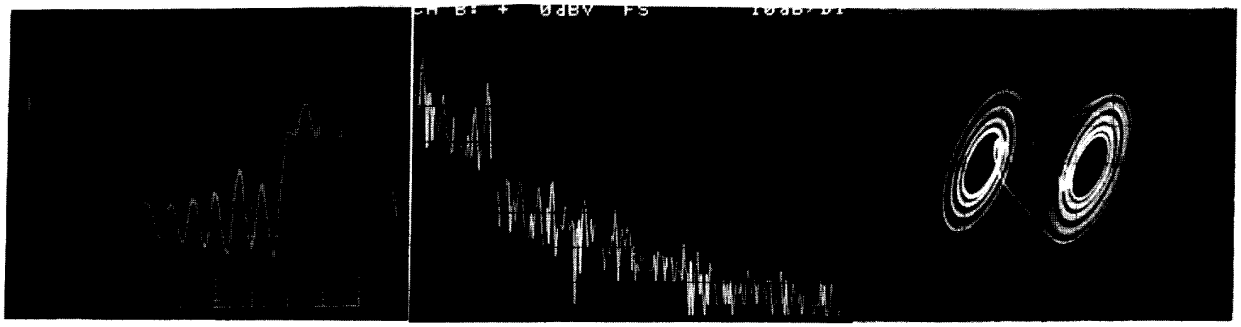

(a) (b) (c)

Figure 21: $R = 1855\Omega$, $C_1 = 10\text{nF}$, $C_2 = 100\text{nF}$, $L = 18\text{mH}$, $m_1 = -\frac{25}{33}\text{mS}$, $m_0 = -\frac{4}{22}\text{mS}$.

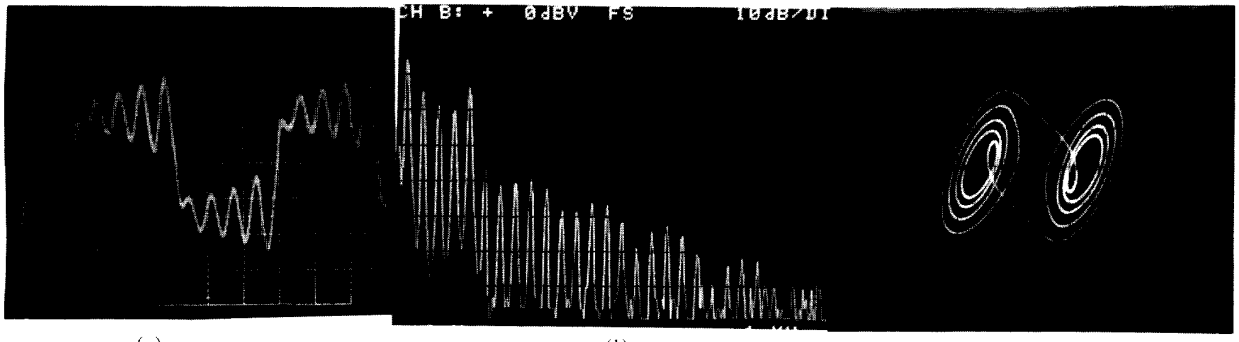

(a) (b) (c)

Figure 22: $R = 1833\Omega$, $C_1 = 10\text{nF}$, $C_2 = 100\text{nF}$, $L = 18\text{mH}$, $m_1 = -\frac{25}{33}\text{mS}$, $m_0 = -\frac{4}{22}\text{mS}$.

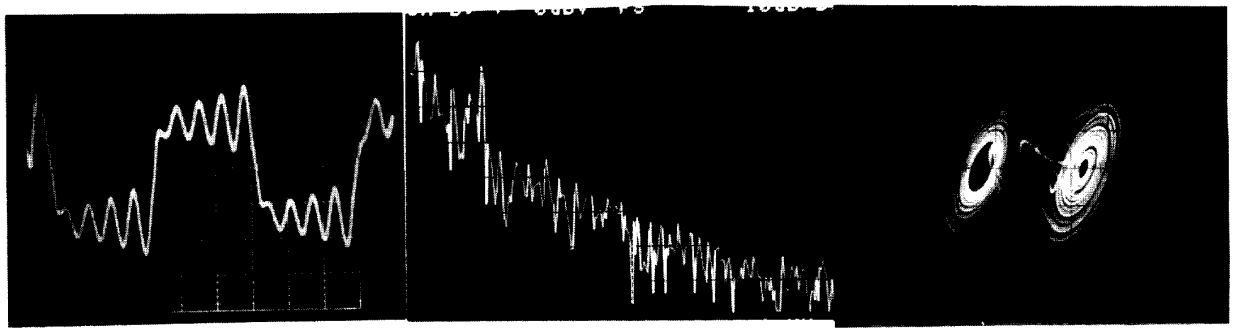

(a) (b) (c)

Figure 23: $R = 1821\Omega$, $C_1 = 10\text{nF}$, $C_2 = 100\text{nF}$, $L = 18\text{mH}$, $m_1 = -\frac{25}{33}\text{mS}$, $m_0 = -\frac{4}{22}\text{mS}$.

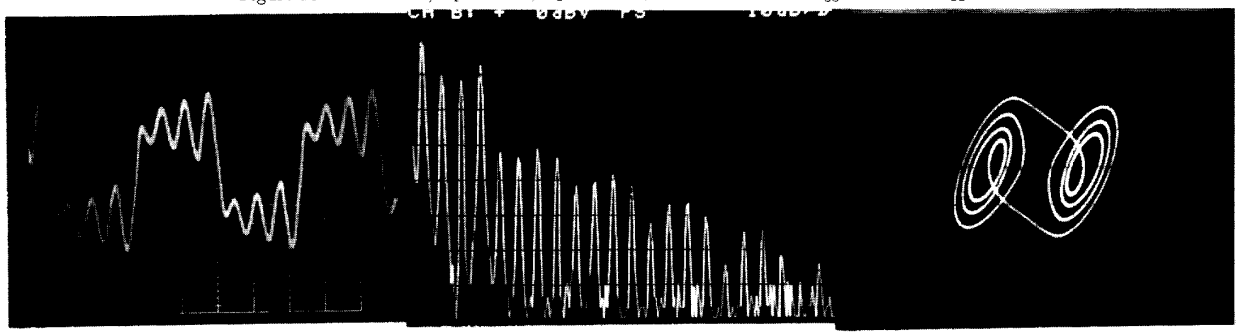

(a) (b) (c)

Figure 24: $R = 1789\Omega$, $C_1 = 10\text{nF}$, $C_2 = 100\text{nF}$, $L = 18\text{mH}$, $m_1 = -\frac{25}{33}\text{mS}$, $m_0 = -\frac{4}{22}\text{mS}$.

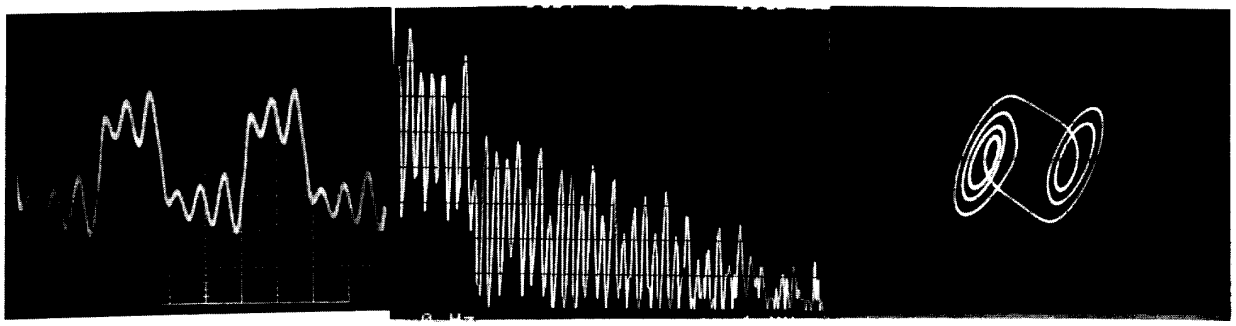

(a) (b) (c)

Figure 25: $R = 1752\Omega$, $C_1 = 10\text{nF}$, $C_2 = 100\text{nF}$, $L = 18\text{mH}$, $m_1 = -\frac{25}{33}\text{mS}$, $m_0 = -\frac{4}{22}\text{mS}$.

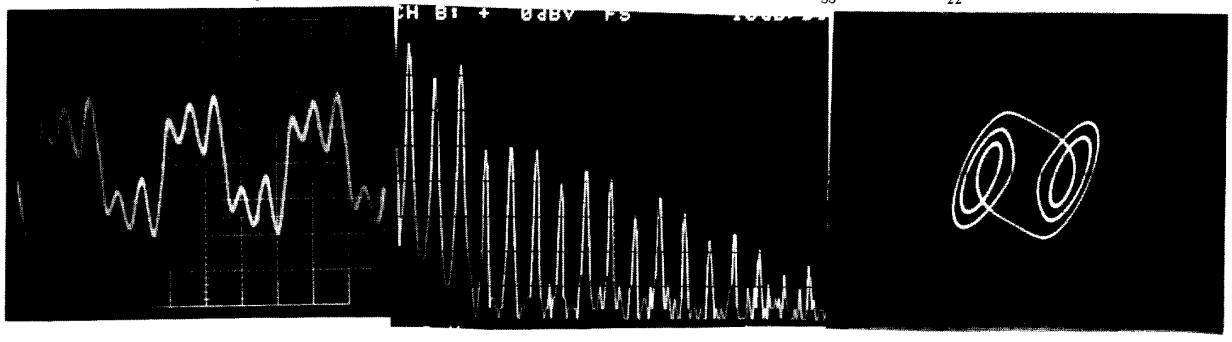

(a) (b) (c)

Figure 26: $R = 1738\Omega$, $C_1 = 10\text{nF}$, $C_2 = 100\text{nF}$, $L = 18\text{mH}$, $m_1 = -\frac{25}{33}\text{mS}$, $m_0 = -\frac{4}{22}\text{mS}$.

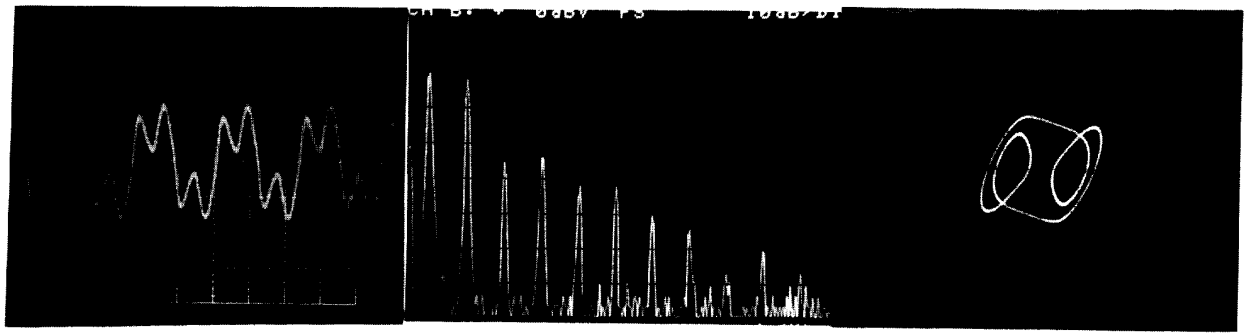

(a) (b) (c)

Figure 27: $R = 1657\Omega$, $C_1 = 10\text{nF}$, $C_2 = 100\text{nF}$, $L = 18\text{mH}$, $m_1 = -\frac{25}{33}\text{mS}$, $m_0 = -\frac{4}{22}\text{mS}$.

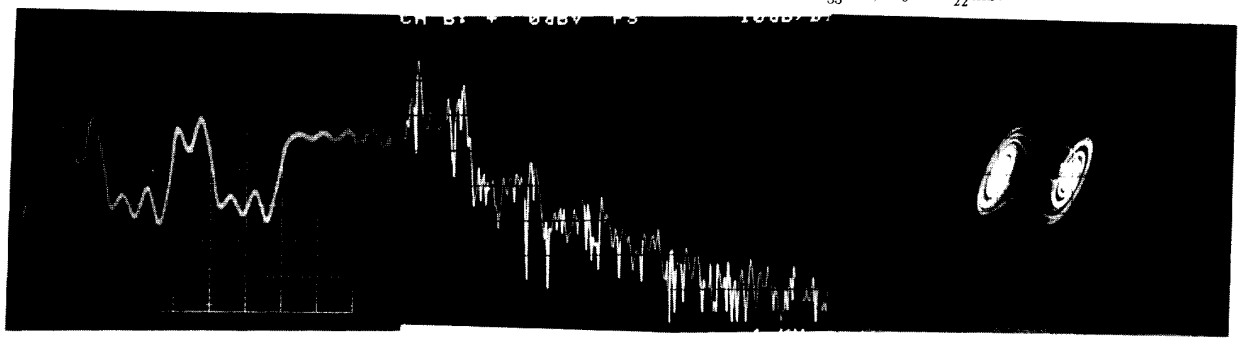

(a) (b) (c)

Figure 28: $R = 1640\Omega$, $C_1 = 10\text{nF}$, $C_2 = 100\text{nF}$, $L = 18\text{mH}$, $m_1 = -\frac{25}{33}\text{mS}$, $m_0 = -\frac{4}{22}\text{mS}$.

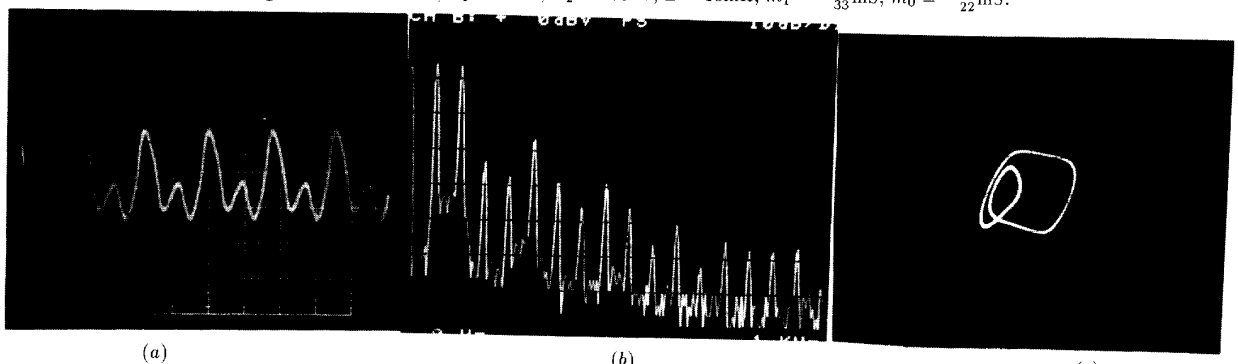

(a) (b) (c)

Figure 29: $R = 1572\Omega$, $C_1 = 10\text{nF}$, $C_2 = 100\text{nF}$, $L = 18\text{mH}$, $m_1 = -\frac{25}{33}\text{mS}$, $m_0 = -\frac{4}{22}\text{mS}$.

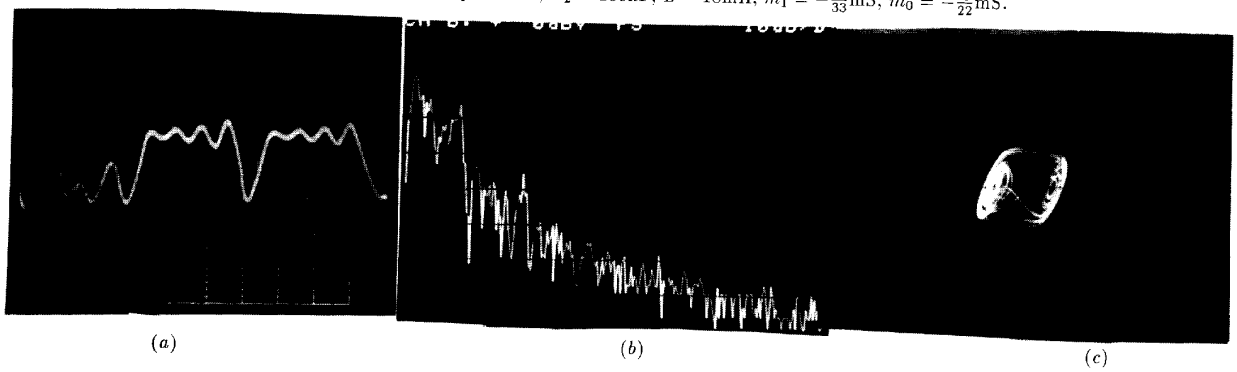

(a) (b) (c)

Figure 30: $R = 1545\Omega$, $C_1 = 10\text{nF}$, $C_2 = 100\text{nF}$, $L = 18\text{mH}$, $m_1 = -\frac{25}{33}\text{mS}$, $m_0 = -\frac{4}{22}\text{mS}$.

Because of symmetry, there are two equilibrium points lying symmetrically with respect to the origin. This is shown in Fig. 7. Similarly, Fig. 8 shows two Rössler attractor sitting symmetrically with respect to the origin. In Fig. 9 to Fig. 30, we see how the right equilibrium point in Fig. 7. is bifurcated into limit cycles and chaotic attractors. For all these figures except Fig. 15 and Fig. 17, in part (a) the scale is 2V/div in the X-axis and 0.5V/div in the Y-axis, and in part (c) the scale in the Y-axis is 2V/div. For Fig. 15 and Fig. 17, in part (a) the scale is 0.5V/div in the X-axis and 0.25V/div in the Y-axis, and in part (c) the scale in the Y-axis is 2V/div. Part (c) of Fig. 15 and Fig. 17 is just Fig. 14 and Fig. 16 expanded to show in more detail the period 4 and period 8 trajectories.

4 From Chua's Circuit to Chua's Oscillator

By inserting a linear resistor R_0 in series with the inductance L in Fig. 1, it is possible to observe many more *strange* attractors, at least 20 of them observed so far, as well as many other bifurcation phenomena (e.g. intermittency), provided the linear circuit elements are also allowed to assume *negative* values. Readers interested in this generalization are referred to the companion article by Chua [14]. To distinguish between this circuit from that of Fig. 1, we will name it *Chua's oscillator* in view of its immense variety of oscillating phenomena.

The significance of Chua's oscillator is its *canonical* property [14]: For every member of a 21-parameter family of odd-symmetric, continuous, piecewise-linear system of ordinary differential equations in $\mathbb{R}^3$ [15, 16], there exists a corresponding set of circuit parameters for Chua's oscillator which exhibits the same qualitative behavior. This fundamental result is quite surprising since Chua's oscillator has only 7 parameters, including the 2 slopes of the 3 odd-symmetric inner segments. Yet it is as general as the 21-parameter family of differential equations.

References

[1] T. Matsumoto, "A chaotic attractor from Chua's circuit," *IEEE Trans. Circuits Syst.*, vol. CAS-31, no. 12, pp. 1055—1058, 1984.

[2] G. Q. Zhong and F. Ayrom, "Experimental confirmation of chaos from Chua's circuit," *Int. J. Circuit Theory Appl.*, vol. 13, no. 11, pp. 93—98, 1985.

[3] G. Q. Zhong and F. Ayrom, "Periodicity and chaos in Chua's circuit," *IEEE Trans. Circuits Syst.*, vol. CAS-32, no. 5, pp. 501—503, 1985.

[4] L. O. Chua, "The genesis of Chua's circuit," *Archiv fur Elektronik und Ubertragungstechnik*, vol. 46, no. 4, pp. 250–257, 1992.

[5] M. P. Kennedy, "Robust op amp realization of Chua's circuit," *Frequenz*, vol. 46, no. 3–4, pp. 66–80, 1992.

[6] R. Madan (Guest Editor), *Special Issue on Chua's Circuit: A Paradigm for Chaos, Part I*, vol. 2 of *Journal of Circuit, Systems, and Computers*. 1993. (To appear in March 1993).

[7] R. Madan (Guest Editor), *Special Issue on Chua's Circuit: A Paradigm for Chaos, Part II*, vol. 2 of *Journal of Circuit, Systems, and Computers*. 1993. (To appear in June 1993).

[8] L. O. Chua, "Graphical analysis and sythesis of memoryless nonlinear networks," in *IEEE International Convention Record, Part 7*, pp. 224–232, 1966.

[9] L. O. Chua, "The rotator–a new network component," *Proceedings of the IEEE*, vol. 15, pp. 1566–1577, Sept. 1967.

[10] L. O. Chua, "Analysis and synthesis of multivalued memoryless nonlinear networks," *IEEE Transactions on Circuit Theory*, vol. 15, pp. 192–209, June 1967.

[11] L. O. Chua, "Synthesis of new nonlinear networks elements," *Proceedings of the IEEE*, vol. 56, pp. 1325–1340, Aug. 1968.

[12] L. O. Chua, *Introduction to Nonlinear Network Theory*. McGraw-Hill, 1970.

[13] J. M. Cruz and L. O. Chua, "A CMOS IC nonlinear resistor for Chua's circuit," ERL memorandum no. m92/16, Electronics Research Laboratory, University of California at Berkeley, CA 94720, February 1992.

[14] L. O. Chua, "A zoo of strange attractors from Chua's circuit," in *Proc. of the 35th Midwest Symposium on Circuits and Systems, Washington DC*, August 9-12 1992.

[15] L. O. Chua, M. Komuro, and T. Matsumoto, "The Double Scroll family, parts I and II," *IEEE Trans. Circuits Syst.*, vol. CAS-33, no. 11, pp. 1073—1118, 1986.

[16] S. Wu, "Chua's circuit family," *Proc. IEEE*, vol. 75, no. 8, pp. 1022—1032, 1987.